Palaeogeography, Palaeoclimatology, Palaeoecology 670 (2025) 112954

Contents lists available at ScienceDirect

Palaeogeography, Palaeoclimatology, Palaeoecology

journal homepage: www.elsevier.com/locate/palaeo

Shell sclerochronology of the limpet *Patella ferruginea* Gmelin, 1791: Implications for growth patterns and reconstruction of past sea surface temperatures

Igor Gutiérrez-Zugasti [a,*], Roberto Suárez-Revilla [a], Asier García-Escárzaga [b], Leon J. Clarke [c], Bernd R. Schöne [d], Jara Pascual-Revilla [a], José Carlos García-Gómez [e], João Zilhão [f], Josefina Zapata [g], Arnaldo Marín [h]

[a] Instituto Internacional de Investigaciones Prehistóricas de Cantabria (Universidad de Cantabria, Gobierno de Cantabria, Banco Santander), Avda. de los Castros, 52, 39005 Santander, Spain
[b] Department of Prehistory and Institute of Environmental Science and Technology (ICTA-UAB), Universitat Autònoma de Barcelona, Bellaterra, Spain
[c] Department of Natural Sciences, Faculty of Science and Engineering, Manchester Metropolitan University, M1 5GD Manchester, UK
[d] Institute of Geosciences, Johannes Gutenberg University, Johann-Joachim-Becher-Weg 21, 55128 Mainz, Germany
[e] Laboratorio de Biología Marina (Dpto. Zoología), Facultad de Biología, Universidad de Sevilla, C/Profesor García González, s/n, 41012 Sevilla, Spain
[f] UNIARQ Centro de Arqueologia da Universidade de Lisboa, Faculdade de Letras, Universidade de Lisboa, Alameda da Universidade, 1600-214 Lisboa, Portugal
[g] Departamento de Zoología y Antropología Física, Facultad de Biología, Universidad de Murcia, Campus de Espinardo, 30100, Murcia, Spain
[h] Departamento de Ecología e Hidrología, Facultad de Biología, Universidad de Murcia, Campus de Espinardo, 30100 Murcia, Spain

ARTICLE INFO

Editor: A. Prendergast

Keywords:
Oxygen stable isotopes
Shells
Molluscs
Oceanography
Archaeology

ABSTRACT

Understanding the environmental conditions faced by past human populations is essential to understand their behaviour, and the subsistence strategies that they adopted for survival. The study of oxygen isotope ratios in limpet shells ($\delta^{18}O_{shell}$) can provide important information on sea surface temperature (SST), shell growth patterns and the season of shell collection by human populations. Following this approach, in this paper, we assessed $\delta^{18}O_{shell}$ values of three modern limpets *Patella ferruginea* Gmelin, 1791 collected alive in Ceuta (northern Africa) as proxies for past SST and to determine the season of shell collection at archaeological sites. Studied shells showed fast growth rates without long periods of growth stops. However, results suggested that the shells did not grow during all tidal immersions. Results also showed higher growth rates between winter and summer, although each shell exhibited its own distinctive patterns. According to the isotope data, studied limpets deposited calcium carbonate to form their shells with an average offset of +0.34 ‰ from expected equilibrium. This offset was higher in summer (0.56 ‰) and lower in winter (0.18 ‰). Reconstructed sea surface temperature ($SST_{\delta 18O}$) exhibited high correlation with satellite temperature. Considering the variability of the oxygen isotope composition of the seawater ($\delta^{18}O_{sw}$), past $SST_{\delta 18O}$ can be calculated with an uncertainty of +2 °C and −1.4 °C. Our study demonstrates that $\delta^{18}O$ values of *P. ferruginea* can be used to reconstruct SST provided that the $\delta^{18}O_{sw}$ is known. Furthermore, the season of shell collection can be estimated from $\delta^{18}O_{shell}$ curves, which has deep implications for future archaeological investigations.

1. Introduction

Marine molluscs have been collected by humans since the Pleistocene and their shells are found at archaeological sites worldwide (Colonese et al., 2011; Gutiérrez-Zugasti et al., 2011; Ramos-Muñoz et al., 2016). Archaeological molluscs can provide significant information on past human behaviour (e.g., Zilhão et al., 2010; Cortés-Sánchez et al., 2019) and likewise on past climate conditions (Wang et al., 2013; García-Escárzaga et al., 2022). Mollusc shells are mainly composed of calcium carbonate ($CaCO_3$) and are precipitated close to oxygen isotopic equilibrium with the surrounding environment (Epstein et al., 1951, 1953; Grossman and Ku, 1986). Hence, during growth, environmental conditions are encoded in the shells, e.g., in the form of stable oxygen isotope ratios ($\delta^{18}O_{shell}$) (Epstein et al., 1951; Dettman et al., 1999).

* Corresponding author.
E-mail address: gutierfi@unican.es (I. Gutiérrez-Zugasti).

https://doi.org/10.1016/j.palaeo.2025.112954
Received 13 December 2024; Received in revised form 8 April 2025; Accepted 9 April 2025
Available online 11 April 2025

The $\delta^{18}O_{shell}$ data record both the sea surface temperature (SST) and the oxygen isotope composition of the seawater ($\delta^{18}O_{sw}$) (e.g., Wanamaker Jr. et al., 2006). As long as the $\delta^{18}O_{sw}$ signature is known, $\delta^{18}O_{shell}$ values of ancient shells can be used for the reconstruction of past SST with sub-monthly resolution (Prendergast et al., 2017). In addition, $\delta^{18}O_{shell}$ profiles can be used in archaeological studies to determine the seasonality of marine mollusc collection, providing information on subsistence strategies and settlement patterns of past human societies (Mannino et al., 2003; Colonese et al., 2009; Burchell et al., 2013; García-Escárzaga et al., 2019).

To test whether $\delta^{18}O_{shell}$ values of a specific taxon can be used as a reliable environmental proxy, an analysis using modern specimens of the selected species is required (e.g., Fenger et al., 2007; Hallmann et al., 2009; Prendergast et al., 2013; Gutiérrez-Zugasti et al., 2017). Moreover, molluscan life cycles are complex and information on shell growth patterns (rate of seasonal shell formation and growth cessation) is also crucial for a correct interpretation of isotope data. Shell growth rate may be modulated by endogenous rhythms, physiology, or environmental factors (e.g., water temperature, salinity, storms, spawning, etc.) (e.g., Schöne, 2008). Calibration of modern limpet specimens of *Patella* spp. such as *P. vulgata* (Fenger et al., 2007; Gutiérrez-Zugasti et al., 2017), *P. caerulea*, *P. rustica* (Ferguson et al., 2011; Prendergast and Schöne, 2017), *P. depressa* (García-Escárzaga et al., 2020) and *P. candei crenata* (Parker et al., 2017), as well as specimens of *Nacella* spp. (Nicastro et al., 2020), have shown the potential of limpets for reconstructing past environmental conditions. Some of these studies have reported the occurrence of a systematic offset from isotopic equilibrium (e.g., Fenger et al., 2007; Ferguson et al., 2011; Nicastro et al., 2020). This offset is species-specific (different between taxa), but also regional (different between localities), suggesting that physiological responses of limpets might be environmentally driven (Gutiérrez-Zugasti et al., 2017).

The limpet *Patella ferruginea* is an endemic marine gastropod of the western Mediterranean Sea that inhabits in the upper intertidal rocky shore. As other limpet species, *P. ferruginea* is present in shell assemblages from Palaeolithic and Neolithic sites along both sides of the Gibraltar strait (North Africa and South Europe), which denotes its early use for human consumption (e.g., Zilhão et al., 2010; Colonese et al., 2011; Ramos-Muñoz et al., 2016; Espinosa et al., 2024). The Gibraltar region is in a privileged geographic position for long-term cultural interactions between Africa and Europe and it is considered a key region in the history of human evolution. Nowadays, *P. ferruginea* is in danger of extinction and is included in the list of the International Union for Conservation of Nature (*International Union for Conservation of Nature,* 2012), the European Council Directive 92/43/EEC on the Conservation of Natural Habitat of Wild Fauna and Flora (1992) and the Spanish Catalogue of Threatened Species in danger of extinction that require strict legal protection (Ley 42/2007, de 13 de diciembre, del Patrimonio Natural y de la Biodiversidad). The decline of this species has been attributed to human impact, mainly during the second half of the 20th century, and it has been related with harvesting, habitat degradation, development of coastal infrastructures and marine pollution (Paracuellos et al., 2003; García-Gómez et al., 2023).

In this paper, we aim to test whether modern specimens of *P. ferruginea* are reliable climate recorders through the study of oxygen isotope ratios of shells collected at Ceuta (northern Africa). Results are used to discuss shell growth patterns, isotopic equilibrium fractionation, and reconstruction of SST. Calibration of *P. ferruginea* $\delta^{18}O_{shell}$ values as a proxy for seawater temperature in northern Africa is crucial to understand environmental conditions experienced by past human societies, and for reconstruction of human subsistence strategies and settlement patterns. Moreover, a more precise knowledge of growth patterns can be useful to protect this species and recover populations.

2. Study area and environmental setting

The autonomous administrative city of Ceuta is a Spanish territory located in North Africa, more specifically, in the Gibraltar Strait. Both African and European shores of the Strait are currently separated by ~14 km of water that connect the Atlantic Ocean with the Mediterranean Sea (Fig. 1A). The coast of Ceuta, about 20 km long, is composed of heterogeneous environments due to the configuration of the coast, as well as by intense port activity. At least 70 % of Ceuta's coast is hard bottom. Of this, ca. 45 % is formed by natural rocky shores (sandstone) and the remaining 25 % are artificial jetties and breakwaters (limestone). These surfaces are inhabited by *P. ferruginea* with a mean density of 0.67 individuals per square meter (Guerra-García et al., 2004).

The climate in the area is Mediterranean with dry summers, and mild and humid winters. Between 2003 and 2010, the mean air temperature ranged between 13.4 °C (January) and 25 °C (August) and rarely dropped below 11 °C or rose above 30 °C. Annual rainfall equalled around 850 mm. Rainfall is markedly seasonal and concentrated from autumn to spring as opposed to very arid summers (Spanish National Meteorological Agency, www.aemet.es).

From an oceanographic point of view, two overlapping ocean currents balance the flows between the Atlantic Ocean and the Mediterranean Sea in the Gibraltar Strait. The current from the Mediterranean Sea runs along the seabed toward the Atlantic Ocean due to its greater density, while the Atlantic current enters the Mediterranean Sea on the surface. Between 2010 and 2014, mean seawater temperature at Ceuta ranged between 14.5 and 23.3 °C. Salinity was constant at around 36 PSU throughout the year (data taken from Copernicus interpolated satellite estimates: Mediterranean Sea - High Resolution L4 Sea Surface Temperature Reprocessed, https://marine.copernicus.eu/).

3. Biology and ecology of *Patella ferruginea*

At present, *P. ferruginea* inhabits a few restricted areas of the Western Mediterranean, including Ceuta and Melilla (Spain), the Chafarinas Islands (Spain), some areas of Morocco, Algeria and Tunisia, the southern Iberian Mediterranean coast, some parts of the Italian peninsula, Corsica, and Sardinia (Rivera-Ingraham et al., 2011; Espinosa et al., 2014). This limpet species is absent at the Atlantic coast of North Africa and the Iberian Peninsula but occurs in the Gibraltar Strait (Fig. 1A). *P. ferruginea* inhabits rocky shores and upper intertidal areas, where the algal coverage is reduced, and a microbial film of diatoms, cyanobacteria, and propagules of other algae predominate, on which this limpet feeds (Guallart and Templado, 2012).

P. ferruginea is a slow-growing limpet with a lifespan between eight and 35 years (Espinosa et al., 2008). It is a large species that can exceed 100 mm in length, although its usual size ranges between 70 and 80 mm. The reproductive period takes place in autumn (Frenkiel, 1975). Between January and July there is complete sexual rest. Gonadal maturation begins at the end of August and the gametes are expelled into the sea (spawning) coinciding with the storms of November (Espinosa et al., 2006; Guallart and Templado, 2012). Following previous investigations, growth has a marked seasonal component, but with differences between localities. In Ceuta, Espinosa et al. (2008) observed higher growth rates in spring-summer than in autumn-winter, while Guallart et al. (2012) reported fastest growth in winter-spring at the Chafarinas Islands. At this locality, growth slows down during summer and autumn because of the higher insolation and the breeding season, respectively. At Ceuta, Rivera-Ingraham et al. (2011) observed faster growth rates in smaller than in bigger specimens. While shells with a length of 2 cm showed growth rates of 1.15–1.68 cm/year, shells with a length of 8 cm exhibited growth rates of 0.38–0.73 cm/year.

4. Material and methods

4.1. Materials: modern shells

Three specimens of *P. ferruginea* were collected alive on 23 October 2014 at the intertidal rocky shore of Cala del Desnarigado (Ceuta, Spain)

Fig. 1. A: Location of Ceuta and the Strait of Gibraltar region. The red areas indicate the current distribution of *P. ferruginea*. B: Location of Cala del Desnarigado, the beach where *P. ferruginea* specimens were collected in October 2014. (For interpretation of the references to colour in this figure legend, the reader is referred to the web version of this article.)

(Fig. 1B) under authorised research directed by one of us (JCGG). Limpets were labelled PF.CT.01, PF.CT.02 and PF.CT.10 (Figs. S1, S2, S3). The soft parts of the limpets were removed with a scalpel immediately after collection to prevent animals from secreting additional shell carbonate. The shells were cleaned with deionised water for 5 min and air-dried at ambient temperature. Length, width, and height of each shell were measured with a digital calliper to the nearest 10 μm. The size of the limpets equalled around 60 mm in length, so they can be considered mature (Table S1).

4.2. Shell carbonate sampling procedure

Following the procedure published by Schöne et al. (2005), two thick-sections were obtained from each limpet (Fig. 2A–B; Figs. S1, S2, S3). The limpet shells were first mounted on metal cubes with Araldite epoxy resin and then coated with a metal epoxy resin (JB Kwik-Weld) along the axis of maximum growth to avoid shell fracturing during the cutting process using a Buehler IsoMet low-speed saw (Buehler IsoMet 1000; operated at 250 rpm) and a 0.5 mm thick diamond-coated saw blade. The two thick-sections of the shell were glued onto microscope glass slides with metal epoxy resin and ground on glass surfaces with F600 and F800 SiC grit powder for 5 and 3 min, respectively. Then, each section was polished with 1 μm Al_2O_3 powder on a Buehler 8″ micro cloth until the internal growth lines and increments were visible. After each grinding and polishing step, specimens were cleaned in an ultrasonic bath with de-ionized water.

For growth pattern analysis, one polished section of each specimen was immersed in Mutvei's solution at 37–40 °C for 20 min under

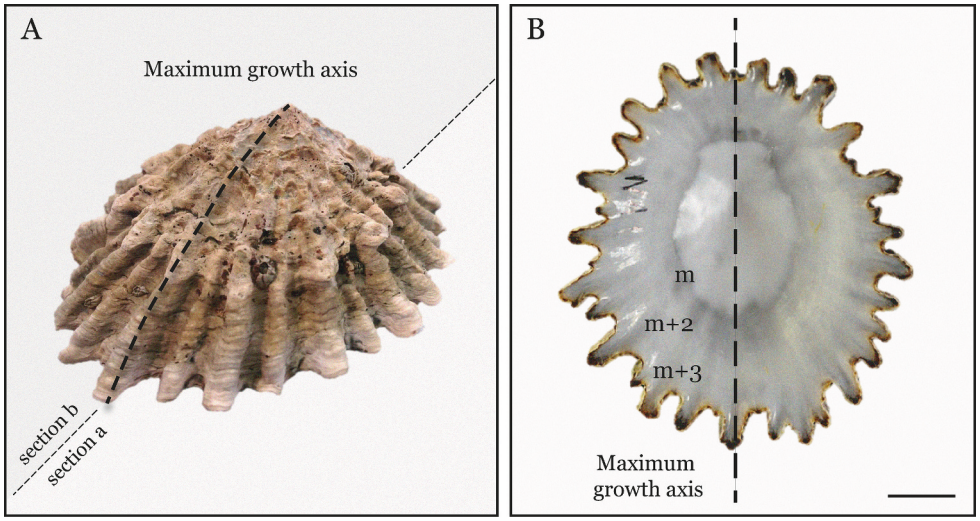

Fig. 2. A) Whole limpet shell of *P. ferruginea* showing the cutting line along the major growth axis (dashed line). Two sections were obtained (section a and b) for isotope and growth pattern analysis respectively; B) Inner surface of the limpet shell showing the different layers of the shell (m, m + 2, m + 3) and the cutting axis. Scale bar = 1 cm.

constant stirring following Schöne et al. (2005). The sections were then gently rinsed in ultra-pure water and air-dried. The use of Mutvei's solution enhanced the visibility of shell growth structures by staining sugars and glycoproteins with Alcian blue which are generally more concentrated at growth lines. Consequently, growth lines appear darker blue than the growth increments between adjacent growth lines (Schöne et al., 2005) (Fig. 3A–C). This allows growth increments and lines to be easily distinguished from each other when observed under the microscope. The stained sections were studied with a Leica S8APO stereoscopic microscope (8–50 × magnification) using sectoral dark-field illumination and a Leica DM 2500 M optical microscope (50–100 × magnification) using reflected light. In both cases, a Leica MC190HD digital camera (10 MP) was used to take photographs.

The remaining polished section of each limpet was used for oxygen isotope analysis (Fig. 3B). Carbonate samples were extracted from the outer concentric cross-foliated (m + 2) and radial crossed foliated (m + 3) calcite layers (MacClintock, 1967) (Fig. 2B). These layers were targeted to avoid the mixture between calcite and aragonite layers following the procedure established by Fenger et al. (2007).

Milling was conducted from the shell aperture toward the apex (i.e., from most recently formed shell portions to older shell portions) using a Micromill (New Wave Research) equipped with a 1 mm conical dental drill bit (H97 104 010; Komet/Brasseler). Sampling followed the shape of the growth lines from the outer to the inner surface of the limpet (Fig. 3D). One hundred carbonate samples were taken from each limpet shell. Despite the high number of micromilled samples, the apex was not reached in any case, so the younger portions of the shells remained unsampled. Each carbonate sample weighed ca. 200 μg. The milled carbonate powder was loaded into 12 ml Exetainers, and $\delta^{18}O_{shell}$ values were measured in a Thermo Finnigan MAT 253 dual inlet isotope ratio mass-spectrometer coupled to a Finnigan Kiel IV carbonate device at the Geoscience Institute CSIC-UCM (Madrid, Spain). A two-point calibration

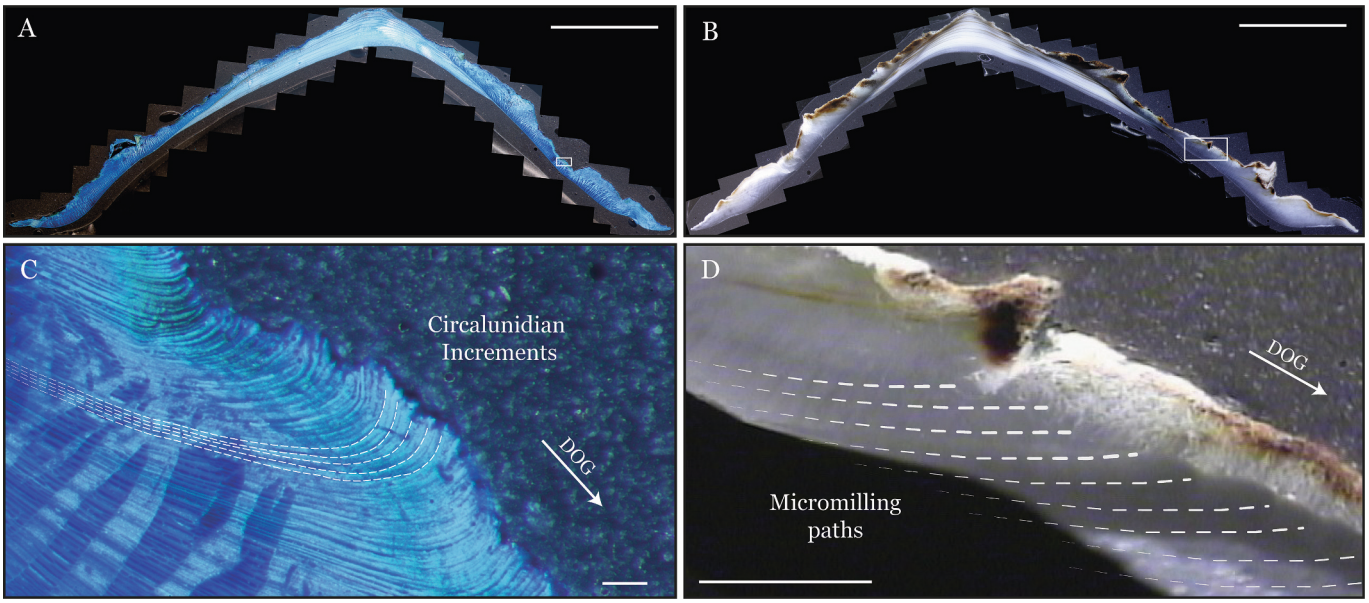

Fig. 3. Sampling strategies in *P. ferruginea*: A) Mutvei-stained shell section used for growth pattern analysis. Scale bar = 1 cm; B) Polished cross-section used for isotope sampling. Scale bar = 1 cm; C) Portion of stained cross-section displaying lunar daily (circalunidian) growth lines (dashed). Scale bar = 100 μm. DOG: direction of growth; E) Posterior portion of polished cross-section showing micromilling paths. Scale bar = 1 mm. DOG = direction of growth.

(NBS-18: $\delta^{18}O = -23.2$ ‰; NBS-19: $\delta^{18}O = -2.2$ ‰) was used to compute $\delta^{18}O_{shell}$ values. The analytical precision of the instrument was better than ±0.04 ‰.

4.3. Shell growth patterns

Mutvei-stained sections were analysed to study shell growth patterns, and especially to identify periods of shell growth slowdown or cessation. The number of lunar days per growing season was calculated from the number of circalunidian growth lines and increments (Fig. 3C) previously produced for *Patella* species to identify the duration of the period of slow growth or even growth cessation (Gutiérrez-Zugasti et al., 2017). The Panopea image processing software (© Peinl and Schöne) was used to count circalunidian growth increments and measure their width to the nearest 1 μm. Age-related growth trends were removed from the increment chronologies following the procedure reported by Schöne (2003). After measuring each circalunidian increment, a series of digital filters available in the statistics software PAST 3.21 (Hammer et al., 2001) was used to explore low, medium, and band-pass signals within the growth increment time-series (Schöne, 2013; Colonese et al., 2013). We used the number of lunar daily (circalunidian) increments to estimate the time represented by each isotope sample. Calendar alignment of the shell oxygen isotope record was achieved with fortnightly and circalunidian growth patterns, starting from the collection day as a reference for anchoring the first $\delta^{18}O_{shell}$ value.

4.4. Reconstruction of sea surface temperature

The $\delta^{18}O_{shell}$ value reflects both changes of SST and $\delta^{18}O_{sw}$. Accordingly, to compute SST from $\delta^{18}O_{shell}$, the $\delta^{18}O_{sw}$ must be known. A 1 ‰ shift in $\delta^{18}O_{sw}$ corresponds to a change in temperature of more than 4 °C (Friedman and O'Neil, 1977). In this paper, we used the average $\delta^{18}O_{sw}$ value of 1.27 ‰ (VSMOW) recorded by Ferguson et al. (2011) in Gibraltar between March 2006 and November 2007. Seawater temperature was then computed by using the fractionation equation by Friedman and O'Neil (1977) for low-Mg calcite:

$$1000ln\alpha = \frac{2.78 \times 10^6}{T^2 - 2.89} \quad (1)$$

where T is the temperature measured in Kelvin and α is the fractionation between water and calcite described by the equation:

$$\alpha = \frac{1000 + \delta^{18}O_{shell}\ (VSMOW‰)}{1000 + \delta^{18}O_{sw}(VSMOW‰)} \quad (2)$$

$\delta^{18}O_{shell}$ (V-PDB ‰) values were converted to the V-SMOW ‰ scale using the equation by Coplen (1988):

$$\delta^{18}O\ VSMOW‰ = 1.03091 \times \delta^{18}O\ VPDB‰ + 30.91 \quad (3)$$

Satellite seawater temperatures along the coast of Ceuta (02 January 2011 to 23 October 2014 = collection date) were obtained from COPERNICUS satellite High Resolution L4 Sea Surface Temperature Reprocessed (https://marine.copernicus.eu/).

5. Results

5.1. Shell growth patterns

Growth pattern analysis was conducted on Mutvei-stained sections of the limpets. Only circalunidian and fortnightly growth patterns were observed, but no major (annual) growth lines. Lunar daily growth increments were separated from each other by (circalunidian) growth lines (Fig. 3C). As in previous sclerochronological studies carried out on limpets (García-Escárzaga et al., 2020; Gutiérrez-Zugasti et al., 2017; Fenger et al., 2007), the width of these lunar daily growth patterns varied periodically and formed bundles containing ca. 14–15 of these microgrowth increments and lines. These bundles are referred to as fortnightly growth patterns and allowed us to place the shell record in a precise temporal context.

As indicated by growth pattern analysis, most of the isotope samples provided sub-monthly to sub-weekly resolution. Actually, samples represented between one and 78 days of growth, with an average between six and ten days per sample (Supplementary data). The shell portions studied for growth patterns were laid down during one and a half and two and a half years. The shells were growing between 67 and 78 % of their lifetime, while growth was significantly retarded or even stopped during the remainder. Shells stopped growing intermittently in any season (Table 1; Table S2), but no long periods of growth cessation periods were identified. The widths of circalunidian growth increments (i.e., lunar daily increments width, LDIW) of the limpets ranged between 9 and 55 μm (arithmetic average = 22 μm) for PF.CT.01, between 13 and 70 (arithmetic average = 33 μm) for PF.CT.02 and between 12 μm and 57 μm (arithmetic average = 29 μm) for PF.CT.10. Average LDIW differed between the studied specimens (20–23 μm in PF.CT.01; 27–30 μm in PF.CT.10; 29–37 μm in PF.CT.02). In all three specimens, broader circalunidian increments were formed in winter. In PF.CT.01, growth was fastest in summer followed by spring, while PF.CT.02 grew fastest in spring, while nearly identical growth rates were recorded in the remaining seasons. Specimen PF.CT.10 grew fastest in winter and at similar rate during the other seasons. Absolute growth per year ranged between 4.6 and 7.5 mm. (Table 1; Table S2).

5.2. Measured and predicted $\delta^{18}O_{shell}$

The $\delta^{18}O_{shell}$ values of the three studied shells showed sinusoidal patterns reflecting seasonal changes in seawater temperature. The isotopic ratios near the shell edge (most recently formed shell portion) translated into temperatures that prevailed during the season of death (Fig. 4). Studied shells showed two and three annual isotope cycles. Highest $\delta^{18}O_{shell}$ values ranged between 1.63 and 1.75 ‰, and minimum values between 0.28 and 0.47 ‰, with a mean of 0.97 to 1.12 ‰ (Table 2). A crossplot of measured and predicted $\delta^{18}O_{shell}$ values revealed a strong correlation in the three shells ($R^2 = 0.87$ for PF.CT.01, $R^2 = 0.90$ for PF.CT.02, $R^2 = 0.88$ for PF.CT.10; $p \leq 0.001$ in all cases). A mean $\delta^{18}O$ annual offset of 0.34 ‰ between measured $\delta^{18}O_{shell}$ and predicted $\delta^{18}O_{shell}$ was identified. Detailed growth pattern data was used

Table 1
Seasonal growth data for the three *P. ferruginea* shells analysed in this study.

	% days growing	Average LDIW (mm)	Average growth (mm)	Absolute growth (mm)
PF.CT.01				
Autumn	69	0.020	1.264	2.875
Summer	87	0.022	1.944	5.833
Spring	85	0.022	1.822	5.467
Winter	73	0.023	1.228	3.325
Mean annual	78	0.022	1.565	4.375
Total			6.259	17.500
PF.CT.02				
Autumn	68	0.029	1.711	2.385
Summer	70	0.028	1.703	3.407
Spring	68	0.036	2.189	4.378
Winter	61	0.037	1.707	3.544
Mean annual	67	0.032	1.828	3.428
Total			7.310	13.713
PF.CT.10				
Autumn	82	0.027	1.847	2.663
Summer	60	0.028	1.686	3.371
Spring	74	0.028	1.859	3.717
Winter	77	0.030	2.157	4.314
Mean annual	73	0.029	1.887	3.516
Total			7.548	14.064

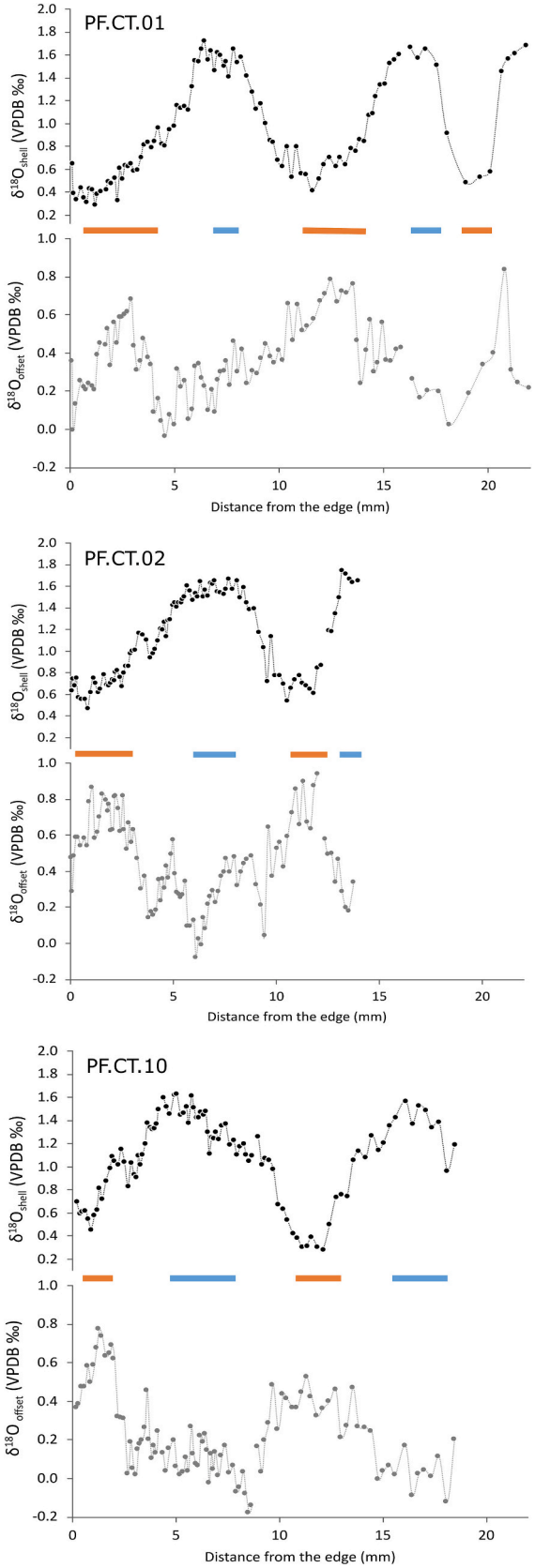

Fig. 4. Isotope profiles ($\delta^{18}O_{shell}$) and offset ($\delta^{18}O_{offset}$) of the three studied shells of *P. ferruginea*. A) PF.CT.01, B) PF.CT.02 and C) PF.CT.10. Blue horizontal lines: winter; Orange horizontal lines: summer. Observe the inverse relationship between $\delta^{18}O_{shell}$ and $\delta^{18}O_{offset}$. (For interpretation of the references to colour in this figure legend, the reader is referred to the web version of this article.)

to analyse the variation of the offset during the different seasons of the year. The average offset was lower during winter (0.18 ‰) and higher in summer (0.56 ‰). Spring and autumn showed intermediate offsets of 0.27 and 0.32 ‰, respectively (Fig. 5; Table 3). The offset showed a sinusoidal pattern in the three shells, following a clear inverse trend with respect to $\delta^{18}O_{shell}$ (Fig. 4). Despite this trend, no correlation was found between $\delta^{18}O_{shell}$ and the $\delta^{18}O_{offset}$ in PF.CT.01 ($R^2 = 0.06$, $p \leq 0.001$), while moderate correlation was found in PF.CT.02 ($R^2 = 0.41$, $p \leq 0.001$) and PF.CT.10 ($R^2 = 0.32$, $p \leq 0.001$).

5.3. Reconstructed SST

The average seasonal offset calculated from the three shells together (Table 3) was subtracted from the measured $\delta^{18}O_{shell}$ to calculate sea surface temperatures ($SST_{\delta18O}$). Once corrected for the average isotope offset, $SST_{\delta18O}$ ranged from 22.3 °C to 14.6 °C (annual range = 7.7 °C). Daily temperatures from the Copernicus satellite ($SST_{satellite}$) during the time span of limpet growth (23 October 2014 to 7 February 2012) ranged between 23.2 °C and 14 °C. Therefore, maximum, and minimum $SST_{\delta18O}$ are 0.9 °C lower and 0.6 °C higher than maximum and minimum $SST_{satellite}$, respectively. However, when $SST_{satellite}$ corresponding to the days represented by each shell carbonate sample were averaged, maximum and minimum $SST_{satellite}$ are 22.2 °C and 14.4 °C (annual range = 7.8 °C), respectively, showing an almost perfect match with maximum and minimum reconstructed $SST_{\delta18O}$ (Table 4). As in the case of measured and predicted $\delta^{18}O_{shell}$, reconstructed $SST_{\delta18O}$ and $SST_{satellite}$, showed very strong correlation (R^2 = 0.90, 0.94 and 0.92, respectively; $p \leq 0.001$) (Fig. 6). A comparison between $SST_{\delta18O}$ and $SST_{satellite}$ showed maximum positive and negative differences of +2.2 °C and −2.5 °C, respectively, although mean values of the whole sample set were between 0.1 and 0.4 °C in the three shells (Supplementary data).

6. Discussion

6.1. Shell growth patterns

Like other gastropods, limpets grow periodically slower and faster resulting in the formation of micrometer-scale growth lines and increments (microgrowth patterns), here circalunidian growth patterns. When combined with oxygen isotope data of the shells, these growth patterns helped to constrain the temporal alignment of the shell record and determine the time represented by each isotope sample. Within any given season, the number of circalunidian increments remained below the expected number of lunar daily increments indicating that limpets stopped growing shell for some time. In fact, there was no particular season during which the shell ceased growing for an extended period of time. The absence of long-term growth stops can explain why no major annual growth lines were developed. Despite growth stops, fortnightly patterns were observed, allowing the temporal alignment of isotope samples.

Ekaratne and Crisp (1982) observed that micro-growth bands in *P. vulgata* formed at each tidal immersion. However, Cudennec and Paulet (2021) observed a large variability in the number of circalunidian increments and lines which led them to suggest that growth may not have occurred during each tidal immersion. The same conclusion may explain the findings herein. The reason for this complex growth pattern is unknown and needs further investigation.

P. ferruginea grows considerably faster than other limpet species, with mean lunar daily increment width ranging between 22 and 33 μm. For comparison, *P. vulgata* grows only half as fast (10 and 13 μm per day; Gutiérrez-Zugasti et al., 2017). Also, the number of lunar days counted

Table 2
Mean, maximum, minimum and range of $\delta^{18}O_{shell}$ values from *P. ferruginea* shells.

Sample ID	$\delta^{18}O$ ‰ (VPDB)				
	n	Max	Min	Mean	Range
PF.CT.01	98	1.73	0.30	0.97	1.43
PF.CT.02	99	1.75	0.47	1.12	1.27
PF.CT.10	98	1.63	0.28	1.09	1.34

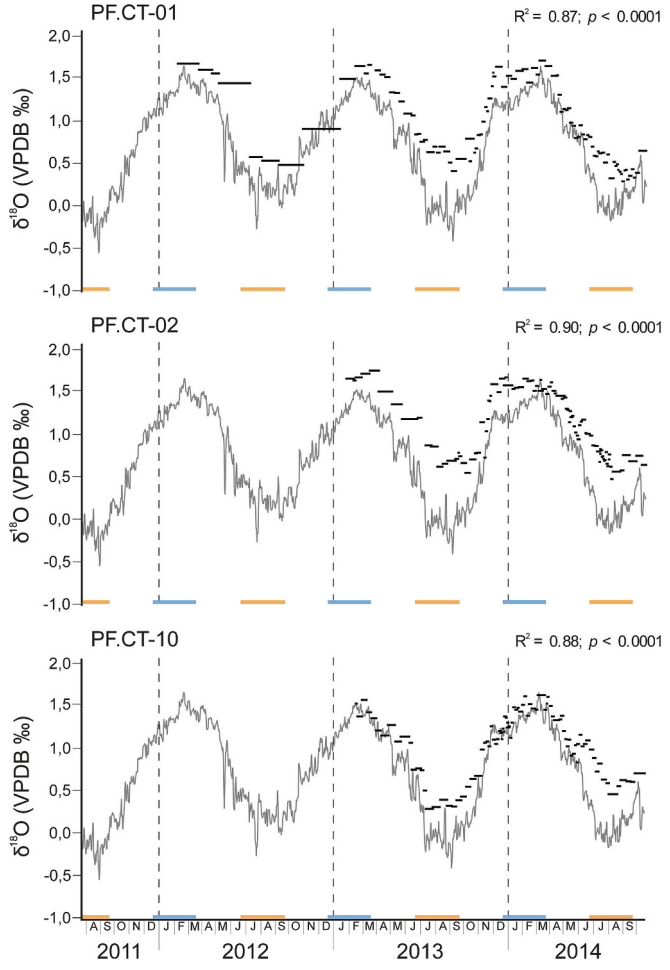

Fig. 5. Calendar-aligned shell oxygen isotope ratios ($\delta^{18}O_{shell}$: horizontal black lines) of specimens PF.CT.01, PF.CT.02 and PF.CT.10. Temporal alignment was achieved considering fortnightly and circalunidian growth patterns. Predicted $\delta^{18}O_{shell}$ values (grey line) were computed from satellite temperature ($SST_{satellite}$) using the mean annual $\delta^{18}O_{sw}$ value and Eqs. (1) and (2). Observe the offset between measured and predicted $\delta^{18}O_{shell}$.

Table 3
Seasonal and annual offset (measured $\delta^{18}O_{shell}$ - predicted $\delta^{18}O_{shell}$) obtained as a function of the sampling sequential methodology in *P. ferruginea*. Data given in ‰ vs VPDB.

Sample ID	Spring	Summer	Autumn	Winter	Mean annual
PF.CT.01	0.28	0.47	0.35	0.22	0.36
PF.CT.02	0.33	0.70	0.42	0.23	0.45
PF.CT.10	0.20	0.51	0.20	0.08	0.22
Average	0.27	0.56	0.32	0.18	0.34

in each time interval is larger in *P. ferruginea* than other species. Based on the findings herein, *P. ferruginea* forms shell during 66–91 % of lunar days per year (Table S2). In *P. vulgata*, this number remains below ca. 60 %. Moreover, *P. ferruginea* grows much faster and thus reaches larger sizes (ca. 60 mm) than *P. vulgata* (ca. 35–38 mm) in a similar time span.

Our data also show some variability in seasonal growth rate between specimens. Average seasonal growth rates varied between the three shells, with higher growth rates in winter, spring or summer, depending on specimen and year (Table S2). These seasons coincide with the periods of sexual rest for this species, suggesting that more energy is available for faster growth during sexual rest and less during the reproduction period (Espinosa et al., 2006; Guallart and Templado, 2012). At Ceuta, Espinosa et al. (2008) reported higher growth rates in this species in spring-summer, while at the Chafarinas Islands faster growth rates occur in winter-spring (Guallart et al., 2012). While in both studies faster growth rates were detected in smaller specimens, no clear ontogenetic trend has been observed in the present study. Very likely this is due to the fact that information on annual growth during 2012 and 2014 is incomplete in our dataset preventing the recognition of ontogenetic trends. Isotope sequences of 2012 and 2014 are likewise incomplete because the specimens were collected before the end of 2014 and younger portions of the shell remained unsampled. This also means that it is not possible to determine the exact age of the specimens. However, given that higher growth rate has been reported for younger individuals, the unsampled portions should represent year one and two at most, suggesting an age of 2.5 to 4.5 years for the specimens analysed in this study. The only complete year of growth was 2013. The width of the respective annual increment differed considerably between specimens (PF.CT0.1: ca. 6.2 mm; PF.CT.02 and PF.CT.10: ca. 7.5 mm). Despite the limitations of the dataset, our results show that the analysed limpets grew fast during their first years of life, at least in comparison with other *Patella* species.

6.2. Oxygen isotope equilibrium

The high correlation between measured and predicted $\delta^{18}O_{shell}$ values suggests that *P. ferruginea* deposited calcium carbonate close to oxygen isotope equilibrium with the surrounding environment. Despite this, the studied shells showed a predictable offset from expected equilibrium, on average, 0.34 ‰ (0.22, 0.36 and 0.45 ‰, respectively, in the three specimens) (Table 3; Supplementary data). Previous investigations of limpets have also reported positive offsets. For example, a 0.36 and 1.01 ‰ offset was reported from *P. vulgata* live-collected from the northern Iberian Peninsula and Great Britain, respectively (Fenger et al., 2007; Gutiérrez-Zugasti et al., 2017). The sclerochronological study of *P. depressa* from northern Iberia also revealed a high positive offset of 1.08 ‰ (García-Escárzaga et al., 2020). Furthermore, a 0.72 ‰ offset was found in *P. caerulea* and *P. rustica* limpets from Gibraltar (Ferguson et al., 2011). Similar offsets have been observed elsewhere: 0.72 ‰ in *P. caerulea* from different Mediterranean locations (Prendergast and Schöne, 2017), 0.70 ‰ in *Patella tabularis* from South Africa (Cohen and Tyson, 1995; Shackleton, 1973) and 1.30 ‰ in *P. candei crenata* from the Canary Islands (Parker et al., 2017). Schifano and Censi (1983) also recorded a positive offset in *P. caerulea* from Sicily (Italy).

The offsets from isotopic equilibrium between measured and predicted $\delta^{18}O_{shell}$ are usually explained by the so-called "vital effects" (i.e., metabolic or biochemical processes). However, their origin is still unknown. Following previous studies (Fenger et al., 2007; Parker et al., 2017), metabolic rather than kinetic fractionation caused the vital effects. These studies explored aspects such as the use of respired CO_2, the changes in the pH of the seawater, the occurrence of evaporative conditions, and the transport of ^{16}O out of the shell during biomineralization. However, they were not able to provide a fully-fledged explanation for the occurrence of the offset. Parker et al. (2017) concluded that the offset is due to internal processes, while Fenger et al. (2007) and Gutiérrez-Zugasti et al. (2017) noted that the influence of external

Table 4
Mean, maximum, minimum and range of reconstructed ($SST_{\delta 18O}$) and satellite ($SST_{satellite}$) temperatures (°C) during shell growth of the three analysed limpets and mean total values.

Sample ID	$SST_{\delta 18O}$				$SST_{satellite}$			
	Mean	Max	Min	Range	Mean	Max	Min	Range
PF.CT.01	18.6	22.5	14.5	8.1	18.6	22.0	14.7	7.4
PF.CT.02	17.9	21.7	14.4	7.3	18.3	22.3	14.2	8.1
PF.CT.10	17.8	22.6	14.9	7.7	17.4	22.3	14.4	7.9
Mean	18.1	22.3	14.6	7.7	18.1	22.2	14.4	7.8

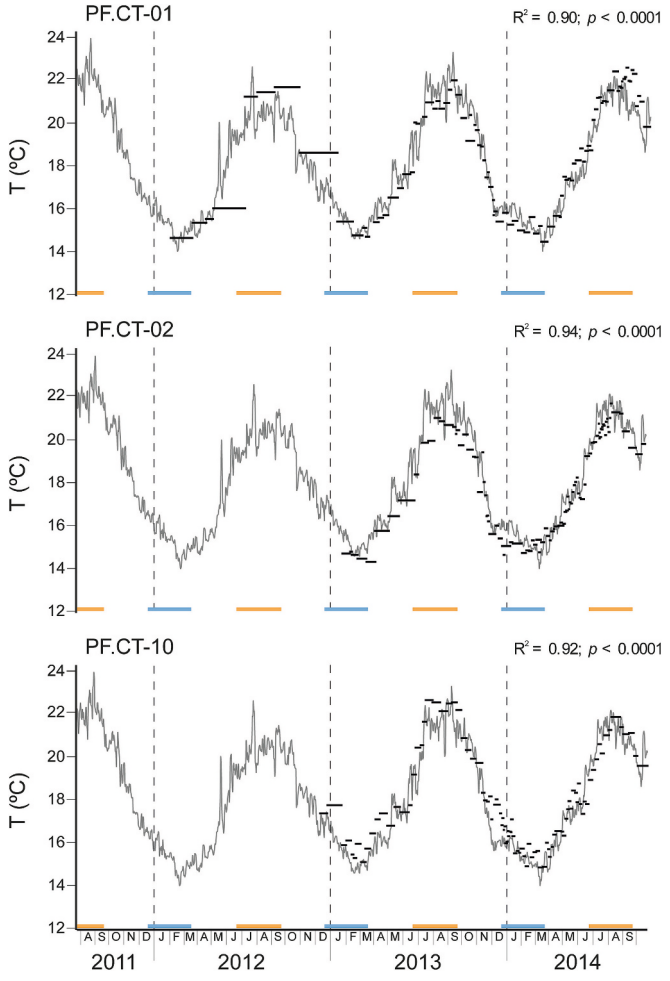

Fig. 6. Reconstructed (seasonal offset corrected) seawater temperatures ($SST_{\delta 18O}$: horizontal black lines) against satellite temperature values ($SST_{satellite}$: grey line) in A) PF.CT.01 ($R^2 = 0.90$; $p \leq 0.001$), B) PF.CT.02 ($R^2 = 0.94$; $p \leq 0.001$) and B) PF.CT.10 ($R^2 = 0.92$; $p \leq 0.001$).

processes, such as $\delta^{18}O_{sw}$ should also be considered.

The offset found in our study (0.34 ‰, corresponding to ca. 1.4 °C) is considerably lower than most reported previously. Seasonal variations of the offset were observed in all shells, with larger offsets during periods of higher SST and vice versa, suggesting that environmental conditions were playing a role in the offset from isotopic equilibrium. Despite that seasonal records of $\delta^{18}O_{sw}$ were not available for Ceuta, a seasonal trend was observed in precipitation during the study period (Fig. S4), with greater rainfall from autumn to spring (with a peak in winter) and evaporation during the drier season (i.e. summer, when precipitation was not recorded at all). Thus, in the absence of major freshwater discharge sources near Cala del Desnarigado (the beach where the *P. ferruginea* shells were collected), seasonal precipitation patterns might be responsible for seasonal changes in $\delta^{18}O_{sw}$ in the area, contributing to modulate the observed seasonal pattern of the offset. In fact, shells of *P. vulgata* from northern Iberia (Gutiérrez-Zugasti et al., 2017) showed a similar pattern of seasonal offsets when predicted $\delta^{18}O_{shell}$ was calculated using the mean annual $\delta^{18}O_{sw}$ but a constant offset throughout the year emerged when seasonal $\delta^{18}O_{sw}$ was used. Other studies using seasonal $\delta^{18}O_{sw}$, as in the cases of *P. depressa* from northern Iberia (García-Escárzaga et al., 2022) and *P. candei crenata* from the Canary Islands (Parker et al., 2017), also reported constant offsets throughout the year, with negligible seasonal differences between measured and predicted values. Therefore, seasonal offsets in limpet shells are caused by changes in $\delta^{18}O_{sw}$ although they can be corrected by using highly resolved $\delta^{18}O_{sw}$ datasets. However, despite this correction, there is still an offset, so other factors are acting in the deviation of $\delta^{18}O_{shell}$ from isotopic equilibrium, as stated by previous studies. In any case, as the offsets are predictable, SST can be calculated by subtracting the offset from $\delta^{18}O_{shell}$. In terms of reconstruction of past SST, average seasonal offsets should be used when only mean annual $\delta^{18}O_{sw}$ is available, as they help to correct the lack of seasonal $\delta^{18}O_{sw}$, providing more accurate results than the mean annual offset.

6.3. Reconstructed seawater temperatures ($SST_{\delta 18O}$)

$SST_{\delta 18O}$ correlated very well with $SST_{satellite}$ corresponding to the days represented by each isotope sample. In fact, they agreed very well with remotely sensed SST, with a maximum mean difference of 0.4 °C when the whole sample set was considered. Although maximum differences of +2.2 and −2.5 °C have been recorded in two samples, most of the samples showed differences of less than 1 °C (Supplementary data). However, when $SST_{\delta 18O}$ were compared with $SST_{satellite}$ throughout the sequence, some differences were observed in summer and winter temperature. Most of the differences were negligible and could be explained by time-averaging issues. However, summer $SST_{\delta 18O}$ recorded by PF.CT.01 and especially PF.CT.02 in 2013 showed offsets of 1–2 °C with respect to daily $SST_{satellite}$. The use of the mean seasonal offset to convert shell oxygen isotope data into seawater temperature likely accounts for some of the differences, but not all. Thus, the cause could be related to short growth stops during which the shell did not record environmental variables. This could be the case for specimen PF.CT.02, that only grew shell during 68 % of the summer. However, specimen PF.CT.01 grew uninterruptedly during the whole season (Table S2) and other environmental factors, such as the absence of seasonal $\delta^{18}O_{sw}$ data and/or preferential growth during periods of optimal conditions (Goodwin et al., 2001), may explain the differences.

The potential impact of the annual $\delta^{18}O_{sw}$ range observed at Gibraltar (0.68 ‰) on the temperature reconstruction was tested by calculating $SST_{\delta 18O}$ using the maximum and minimum $\delta^{18}O_{sw}$ values. Results showed an absolute mean difference of ca. 3 °C (Table 5) and a mean deviation of +1.8 and −1.2 °C, respectively, from the temperatures reconstructed with the mean $\delta^{18}O_{sw}$ (Table S3). When the analytical precision of the IRMS (± 0.2 °C) is considered, results suggest that past $SST_{\delta 18O}$ can be calculated with a maximum uncertainty of +2.0 and −1.4 °C when the extreme $\delta^{18}O_{sw}$ values are used. This uncertainty is slightly lower than those reported for other species such as *Phorcus lineatus*, *P. vulgata* (Gutiérrez-Zugasti et al., 2015; Gutiérrez-Zugasti et al., 2017) and *Phorcus turbinatus* (Prendergast et al., 2013).

Table 5
Mean, maximum, minimum and range of $SST_{\delta 18O}$ using maximum and minimum $\delta^{18}O_{sw}$ values.

	Mean	Max	Min	Range
Reconstructed SST (°C) (Max $\delta^{18}O_{sw}$ = 1.67 ‰)				
PF.CT.01	20.4	24.4	16.2	8.2
PF.CT.02	19.7	23.6	16.4	7.2
PF.CT.10	19.6	24.5	16.6	7.9
Mean	19.9	24.1	16.4	7.7
Reconstructed SST (°C) (Min $\delta^{18}O_{sw}$ = 0.99 ‰)				
PF.CT.01	17.4	21.2	13.3	8.0
PF.CT.02	16.7	20.4	13.2	7.2
PF.CT.10	16.6	21.3	13.7	7.6
Mean	16.9	21.0	13.4	7.6

Despite not all days are represented in the three shells and the potential uncertainties introduced by the $\delta^{18}O_{sw}$, the temperature reconstruction showed that the $\delta^{18}O$ values of *P. ferruginea* reliably reflect satellite SST when using the mean annual $\delta^{18}O_{sw}$ signature and seasonal offsets. Therefore, as in the case of other limpet species, *P. ferruginea* can be used to reconstruct past seawater temperature provided that the past $\delta^{18}O_{sw}$ is known. Moreover, results accurately reflect the season of death of the limpets, which means that $\delta^{18}O_{shell}$ and reconstructed SST can be used to infer the season of collection of limpets collected from archaeological sites. This kind of information can provide crucial information on subsistence strategies and settlement patterns of past human societies.

7. Conclusions

The limpet *Patella ferruginea* is a Mediterranean gastropod in danger of extinction, which has limited the number of replicates of this study to a minimum. Using highly resolved sclerochronological and oxygen stable isotope data, we unlocked relevant biological and environmental information from modern shells from Ceuta (northern Africa). The studied limpet shells showed an almost continuous fast growth during their first years of life. Significant growth cessations were not observed. However, the absence of a strong correlation between the number of days during shell growth and the number of calendar days suggests that the shells did not grow during all tidal immersions. Presumably, this is the result of vital effects or environmental constraints. Results also showed higher growth rates between winter and summer, although each shell exhibited its own distinctive pattern.

Shell oxygen isotope ratios were calibrated against satellite sea surface temperature to establish their reliability as a temperature proxy. Results showed that limpets precipitated carbonate close to expected oxygen isotope equilibrium, with a mean offset of merely 0.34 ‰ (equivalent to ca. 1.4 °C). The seasonal isotope offset was larger in summer (0.56 ‰) than in winter (0.18 ‰), following an inverse seasonal trend with respect to $\delta^{18}O_{shell}$, suggesting that environmental conditions were playing a role in the occurrence of the offset. However, previous studies showed that seasonal offsets are caused by seasonal changes in $\delta^{18}O_{sw}$, and that they can be corrected by using high resolution $\delta^{18}O_{sw}$ data. In the absence of seasonal $\delta^{18}O_{sw}$ the use of seasonal offsets for calculating SST provides more accurate results. In the case of *P. ferruginea*, reconstructed seawater temperatures using the mean seasonal offsets and the mean annual $\delta^{18}O_{sw}$ reported for the Gibraltar Strait exhibited high correlation with satellite temperature. When maximum and minimum $\delta^{18}O_{sw}$ were used, results suggest that past $SST_{\delta 18O}$ can be calculated with a maximum uncertainty of +2.0 and −1.4 °C. Our results also showed that fast-growing species such as *P. ferruginea* can provide higher-resolution SST records than slow-growing species.

Therefore, the isotope information recorded in the shells can be used to infer environmental (and paleoenvironmental) conditions and obtain biological information including ontogenetic age of the specimens (when sampling from the edge to the apex) and seasonal growth rates. Concluding from results herein, $\delta^{18}O_{shell}$ values of *P. ferruginea* serve as a very accurate proxy for SST estimates and to reconstruct the seasonality of shell collection, exhibiting great potential for the study of ancient shells from archaeological sites. However, when using this species for the reconstruction of past SST, the influence of environmental factors, such as the past $\delta^{18}O_{sw}$, must be considered.

The results also emphasise the importance of the combined use of isotope geochemical and sclerochronological methodologies. This approach can contribute to a better understanding and interpretation of the different species of molluscs and especially those taxa that require of greater knowledge, protection and monitoring due to their delicate risk of survival.

CRediT authorship contribution statement

Igor Gutiérrez-Zugasti: Writing – original draft, Methodology, Investigation, Funding acquisition, Formal analysis, Conceptualization. **Roberto Suárez-Revilla:** Writing – original draft, Methodology, Investigation, Formal analysis. **Asier García-Escárzaga:** Writing – review & editing, Methodology, Investigation. **Leon J. Clarke:** Writing – review & editing, Resources, Investigation. **Bernd R. Schöne:** Writing – review & editing, Resources, Investigation. **Jara Pascual-Revilla:** Writing – review & editing, Investigation, Formal analysis. **José Carlos García-Gómez:** Writing – review & editing, Resources, Investigation. **João Zilhão:** Writing – review & editing, Investigation. **Josefina Zapata:** Writing – review & editing, Resources, Investigation, Conceptualization. **Arnaldo Marín:** Writing – review & editing, Resources, Investigation, Funding acquisition, Conceptualization.

Funding

This research was supported by the projects HAR 2017-86262-P, funded by AEI/FEDER, UE and PID2021-124059NB-I00, funded by MICIU/AEI/10.13039/501100011033 and FEDER, UE. Additionally, some parts of the research were funded by the Aquatic Ecology Research Group of the University of Murcia. RSR was supported by a predoctoral grant from the Plan Estatal de Investigación Científica y Técnica y de Innovación 2013–2016 (BES-2014-070075) co-funded by the Ministerio de Economía y Competitividad (MINECO), the Servicio Público de Empleo Estatal and the Fondo Social Europeo at the Instituto Internacional de Investigaciones Prehistóricas de Cantabria (IIIPC) of the Universidad de Cantabria. AGE was funded by the Catalonia Postdoctoral Programme through a Beatriu de Pinós fellowship (2020_BP_00240) and he is currently working in the framework of a Marie Skłodowska Curie Action – Postdoctoral Fellowship (101064225-NEARCOAST, https://doi.org/10.3030/101064225), funded by the European Commission.

Declaration of competing interest

The authors declare that they have no known competing financial interests or personal relationships that could have appeared to influence the work reported in this paper.

Acknowledgements

We thank Javier Martín-Chivelet for his help in some parts of the study. Shells were collected in the framework of the project “Proyectos de generación de conocimiento, translocación y seguimiento de la especie en peligro de extinción *Patella ferruginea*” funded and authorised by OBIMASA (Consejería de Medio Ambiente de la Ciudad Autónoma de Ceuta).

Appendix A. Supplementary data

Supplementary data to this article can be found online at https://doi.org/10.1016/j.palaeo.2025.112954.

Data availability

All data is included in the supplementary files

References

Burchell, M., Cannon, A., Hallmann, N., Schwarcz, H.P., Schöne, B.R., 2013. Refining estimates for the season of shellfish collection on the Pacific Northwest coast: applying high-resolution stable oxygen isotope analysis and sclerochronology. Archaeometry 55, 258–276. https://doi.org/10.1111/j.1475-4754.2012.00684.x.

Cohen, A.L., Tyson, P.D., 1995. Sea-surface temperature fluctuations during the Holocene off the south coast of Africa: implications for terrestrial climate and rainfall. The Holocene 5, 304–312. https://doi.org/10.1177/095968369500500305.

Colonese, A.C., Troelstra, S., Ziveri, P., Martini, F., Lo Vetro, D., Tommasini, S., 2009. Mesolithic shellfish exploitation in SW Italy: seasonal evidence from the oxygen isotopic composition of *Osilinus turbinatus* shells. J. Archaeol. Sci. 36, 1935–1944. https://doi.org/10.1016/j.jas.2009.04.021.

Colonese, A.C., Mannino, M.A., Bar-Yosef Mayer, D.E., Fa, D.A., Finlayson, J.C., Lubell, D., Stiner, M.C., 2011. Marine mollusc exploitation in Mediterranean prehistory: an overview. Quat. Int. 239, 86–103. https://doi.org/10.1016/j.quaint.2010.09.001.

Colonese, A.C., Zanchetta, G., Fallick, A.E., Manganelli, G., Saña, M., Alcade, G., Nebot, J., 2013. Holocene snail shell isotopic record of millennial-scale hydrological conditions in western Mediterranean: data from Bauma del Serrat del Pont (NE Iberian Peninsula). Quat. Int. 303, 43–53. https://doi.org/10.1016/j.quaint.2013.01.019.

Coplen, T.B., 1988. Normalization of oxygen and hydrogen isotope data. Chem. Geol.: Isotope Geoscience section 72, 293–297. https://doi.org/10.1016/0168-9622(88)90042-5.

Cortés-Sánchez, M., Simón-Vallejo, M.D., Jiménez-Espejo, F.J., Lozano Francisco, M.d.C., Vera-Peláez, J.L., Maestro González, A., Morales-Muñiz, A., 2019. Shellfish collection on the westernmost Mediterranean, Bajondillo cave (~160-35 cal kyr BP): a case of behavioral convergence? Quat. Sci. Rev. 217 (284), 296. https://doi.org/10.1016/j.quascirev.2019.02.007.

Cudennec, J.-F., Paulet, Y.-M., 2021. Characterising inter-individual growth variability of *Patella vulgata* shell through calcein marking experiments: consequences for palaeo-environmental studies. Environ. Archaeol. 1-14. https://doi.org/10.1080/14614103.2021.1893586.

Dettman, D.L., Reische, A.K., Lohmann, K.C., 1999. Controls on the stable isotope composition of seasonal growth bands in aragonitic fresh-water bivalves (unionidae). Geochim. Cosmochim. Acta 63, 1049–1057. https://doi.org/10.1016/s0016-7037(99)00020-4.

Ekaratne, S.U.K., Crisp, D.J., 1982. Tidal micro-growth bands in intertidal gastropod shells, with an evaluation of band-dating techniques. Proc. R. Soc. Lond. B 214, 305–323. https://doi.org/10.1098/rspb.1982.0013.

Epstein, S., Buchsbaum, R., Lowenstam, H., Urey, H.C., 1951. Carbonate-water isotopic temperature scale. Geol. Soc. Am. Bull. 62, 417–426. https://doi.org/10.1130/0016-7606(1951)62[417:CITS]2.0.CO;2.

Epstein, S., Buchsbaum, R., Lowenstam, H., Urey, H.C., 1953. Revised carbonate-water isotopic temperature scale. Geol. Soc. Am. Bull. 64, 1315–1326. https://doi.org/10.1130/0016-7606(1953)64[1315:RCITS]2.0.CO;2.

Espinosa, F., Guerra-García, J.M., Fa, D., García-Gómez, J.C., 2006. Aspects of reproduction and their implications for the conservation of the endangered limpet, *Patella ferruginea*. Invertebr. Reprod. Dev. 49, 85–92. https://doi.org/10.1080/07924259.2006.9652197.

Espinosa, F., González, A.R., Maestre, M.J., Fa, D., Guerra-García, J.M., García-Gómez, J. C., 2008. Responses of the endangered limpet *Patella ferruginea* to reintroduction under different environmental conditions: survival, growth rates and life-history. Ital. J. Zool. 75, 371–384. https://doi.org/10.1080/11250000801887740.

Espinosa, F., Rivera-Ingraham, G.A., Maestre, M., González, A.R., Bazairi, H., García-Gómez, J.C., 2014. Updated global distribution of the threatened marine limpet *Patella ferruginea* (Gastropoda: Patellidae): an example of biodiversity loss in the Mediterranean. Oryx 48, 266–275. https://doi.org/10.1017/S0030605312000580.

Espinosa, F., Navarro-Barranco, C., Vázquez-Luis, M., Fa, D., 2024. Extirpation of the currently endangered mollusc *Patella ferruginea* through the Mediterranean during the Pleistocene: a matter of human harvesting or environmental factors? Ann. Paléontol. 110, 102724. https://doi.org/10.1016/j.annpal.2024.102724.

Fenger, T., Surge, D., Schöne, B., Milner, N., 2007. Sclerochronology and geochemical variation in limpet shells (*Patella vulgata*): a new archive to reconstruct coastal sea surface temperature. Geochem. Geophys. Geosyst. 8, Q07001 doi:07010.01029/02006GC001488.E.

Ferguson, J.E., Henderson, G.M., Fa, D.A., Finlayson, J.C., Charnley, N.R., 2011. Increased seasonality in the Western Mediterranean during the last glacial from limpet shell geochemistry. Earth Planet. Sci. Lett. 308, 325–333. https://doi.org/10.1016/j.epsl.2011.05.054.

Frenkiel, L., 1975. Contribution à l'étude des cycles de reproduction des Patellidae en Algérie. Pubbl. Stn. zool. Napoli 39, 153–189.

Friedman, I., O'Neil, J.R., 1977. Compilation of stable isotope fractionation factors of geochemical interest. In: Fleischer, M. (Ed.), Data of Geochemistry. United States Department of the Interior, Washington, pp. 1–12. https://doi.org/10.3133/pp440KK.

García-Escárzaga, A., Gutiérrez-Zugasti, I., Cobo, A., Cuenca-Solana, D., Martín-Chivelet, J., Roberts, P., González-Morales, M.R., 2019. Stable oxygen isotope analysis of *Phorcus lineatus* (da Costa, 1778) as a proxy for foraging seasonality during the Mesolithic in northern Iberia. Archaeol. Anthropol. Sci. 11, 5631–5644. https://doi.org/10.1007/s12520-019-00880-x.

García-Escárzaga, A., Gutiérrez-Zugasti, I., González-Morales, M.R., Arrizabalaga, A., Zech, J., Roberts, P., 2020. Shell sclerochronology and stable oxygen isotope ratios from the limpet *Patella depressa* Pennant, 1777: implications for palaeoclimate reconstruction and archaeology in northern Spain. Palaeogeogr. Palaeoclimatol. Palaeoecol. 560, 110023. https://doi.org/10.1016/j.palaeo.2020.110023.

García-Escárzaga, A., Gutiérrez-Zugasti, I., Marín-Arroyo, A.B., Fernandes, R., Núñez de la Fuente, S., Cuenca-Solana, D., Iriarte, E., Simões, C., Martín-Chivelet, J., González-Morales, M.R., Roberts, P., 2022. Human forager response to abrupt climate change at 8.2 ka on the Atlantic coast of Europe. Sci. Rep. 12, 6481. https://doi.org/10.1038/s41598-022-10135-w.

García-Gómez, J.C., Cid-Iturbe, A., Ostalé-Valriberas, E., Espada, R., Carballo, J.L., Fa, D. A., García-Olaya, C., Blanca-Sújar, R., 2023. Advances in the management and translocation methodology of the endangered mollusk *Patella ferruginea* in artificial habitats of port infrastructures: implications for its conservation. Front. Mar. Sci. 10. https://doi.org/10.3389/fmars.2023.1166937.

Goodwin, D.H., Flessa, K.W., Schöne, B.R., Dettman, D.L., 2001. Cross-calibration of daily growth increments, stable isotope variation, and temperature in the Gulf of California bivalve mollusk *Chione cortezi*: implications for paleoenvironmental analysis. PALAIOS 16, 387–398. https://doi.org/10.1669/0883-1351(2001)016<0387:CCODGI>2.0.CO;2.

Grossman, E.L., Ku, T.-L., 1986. Oxygen and carbon isotope fractionation in biogenic aragonite: temperature effects. Chem. Geol. 59, 59–74. https://doi.org/10.1016/0168-9622(86)90057-6.

Guallart, J., Templado, J., 2012. Patella ferruginea. In: VV.AA., Bases ecológicas preliminares para la conservación de las especies de interés comunitario en España: Invertebrados. Ministerio de Agricultura, Alimentación y Medio Ambiente, Madrid.

Guallart, J., Acevedo, I., Calvo, M., 2012. Estimas de edad y crecimiento de la lapa amenazada *Patella ferruginea* (Mollusca, Patellidae) en las islas Chafarinas (Mediterráneo occidental). Rev. Investig. Mar. 19, 181.

Guerra-García, J.M., Corzo, J., Espinosa, F., García-Gómez, J.C., 2004. Assessing habitat use of the endangered marine mollusc *Patella ferruginea* (Gastropoda, Patellidae) in northern Africa: preliminary results and implications for conservation. Biol. Conserv. 116, 319–326. https://doi.org/10.1016/S0006-3207(03)00201-5.

Gutiérrez-Zugasti, I., Andersen, S.H., Araújo, A.C., Dupont, C., Milner, N., Monge-Soares, A.M., 2011. Shell midden research in Atlantic Europe: State of the art, research problems and perspectives for the future. Quat. Int. 239, 70–85. https://doi.org/10.1016/j.quaint.2011.02.031.

Gutiérrez-Zugasti, I., García-Escárzaga, A., Martín-Chivelet, J., González-Morales, M.R., 2015. Determination of sea surface temperatures using oxygen isotope ratios from Phorcus lineatus (Da Costa, 1778) in northern Spain: implications for palaeoclimate and archaeological studies. The Holocene 25, 1002–1014. https://doi.org/10.1177/0959683615574892.

Gutiérrez-Zugasti, I., Suárez-Revilla, R., Clarke, L.J., Schöne, B.R., Bailey, G.N., González-Morales, M.R., 2017. Shell oxygen isotope values and sclerochronology of the limpet *Patella vulgata* Linnaeus 1758 from northern Iberia: implications for the reconstruction of past seawater temperatures. Palaeogeogr. Palaeoclimatol. Palaeoecol. 475, 162–175. https://doi.org/10.1016/j.palaeo.2017.03.018.

Hallmann, N., Burchell, M., Schöne, B.R., Irvine, G.V., Maxwell, D., 2009. High-resolution sclerochronological analysis of the bivalve mollusk *Saxidomus gigantea* from Alaska and British Columbia: techniques for revealing environmental archives and archaeological seasonality. J. Archaeol. Sci. 36, 2353–2364. https://doi.org/10.1016/j.jas.2009.06.018.

Hammer, O., Harper, D.A.T., Ryan, P.D., 2001. Paleontological statistics software package for education and data analysis. Palaeontol. Electron. 4, 9pp. http://palaeo-electronica.org/2001_2001/past/issue2001_2001.htm.

IUCN Red List Categories and Criteria, Version 3.1, second edition, 2012. International Union for Conservation of Nature. UICN, Gland and Cambridge. https://portals.iucn.org/library/node/10315.

Ley 42/2007, de 13 de diciembre, del Patrimonio Natural y de la Biodiversidad. *Boletín Oficial del Estado,* 299, de 14 de diciembre de 2007 (BOE-A-2007-21490). https://www.boe.es/eli/es/l/2007/12/13/42/con.

MacClintock, C., 1967. Shell structure of patelloid and bellerophontoid Gastropods (mollusca). Bull. Peabody Mus. Nat. Hist. 22. https://elischolar.library.yale.edu/peabody_museum_natural_history_bulletin/22.

Mannino, M.A., Spiro, B.F., Thomas, K.D., 2003. Sampling shells for seasonality: oxygen isotope analysis on shell carbonates of the inter-tidal gastropod *Monodonta lineata* (da Costa) from populations across its modern range and from a Mesolithic site in southern Britain. J. Archaeol. Sci. 30, 667–679. https://doi.org/10.1016/S0305-4403(02)00238-8.

Nicastro, A., Surge, D., Briz i Godino, I., Álvarez, M., Schöne, B.R., Bas, M., 2020. High-resolution records of growth temperature and life history of two *Nacella* limpet species, Tierra del Fuego, Argentina. Palaeogeogr. Palaeoclimatol. Palaeoecol. 540, 109526. https://doi.org/10.1016/j.palaeo.2019.109526.

Paracuellos, M., Nevado, J.C., Moreno, D., Giménez, A., Alesina, J.J., 2003. Conservational status and demographic characteristics of *Patella ferruginea* Gmelin, 1791 (Mollusca, Gastropoda) on the Alboran Island (Western Mediterranean). Anim.

Biodivers. Conserv. 26, 29–37. https://raco.cat/index.php/ABC/article/view/57398.

Parker, W.G., Yanes, Y., Surge, D., Mesa-Hernández, E., 2017. Calibration of the oxygen isotope ratios of the gastropods *Patella candei crenata* and *Phorcus atratus* as high-resolution paleothermometers from the subtropical eastern Atlantic Ocean. Palaeogeogr. Palaeoclimatol. Palaeoecol. 487, 251–259. https://doi.org/10.1016/j.palaeo.2017.09.006.

Prendergast, A.L., Schöne, B.R., 2017. Oxygen isotopes from limpet shells: Implications for palaeothermometry and seasonal shellfish foraging studies in the Mediterranean. Palaeogeogr. Palaeoclimatol. Palaeoecol. 484, 33–47. https://doi.org/10.1016/j.palaeo.2017.03.007.

Prendergast, A.L., Azzopardi, M., O'Connell, T.C., Hunt, C., Barker, G., Stevens, R.E., 2013. Oxygen isotopes from *Phorcus* (*Osilinus*) *turbinatus* shells as a proxy for sea surface temperature in the central Mediterranean: a case study from Malta. Chem. Geol. 345, 77–86. https://doi.org/10.1016/j.chemgeo.2013.02.026.

Prendergast, A.L., Versteegh, E.A.A., Schöne, B.R., 2017. New research on the development of high-resolution palaeoenvironmental proxies from geochemical properties of biogenic carbonates. Palaeogeogr. Palaeoclimatol. Palaeoecol. 484, 1–6. https://doi.org/10.1016/j.palaeo.2017.05.032.

Ramos-Muñoz, J., Cantillo-Duarte, J.J., Bernal-Casasola, D., Barrena-Tocino, A., Domínguez-Bella, S., Vijande-Vila, E., Clemente-Conte, I., Gutiérrez-Zugasti, I., Soriguer-Escofet, M., Almisas-Cruz, S., 2016. Early use of marine resources by Middle/Upper Pleistocene human societies: the case of Benzú rockshelter (northern Africa). Quat. Int. 407, 6–15. https://doi.org/10.1016/j.quaint.2015.12.092.

Rivera-Ingraham, G.A., Espinosa, F., García-Gómez, J.C., 2011. Conservation status and updated census of *Patella ferruginea* (Gastropoda, Patellidae) in Ceuta: distribution patterns and new evidence of the effects of environmental parameters on population structure. Anim. Biodivers. Conserv. 34, 83–99. https://raco.cat/index.php/ABC/article/view/243396.

Schifano, G., Censi, P., 1983. Oxygen isotope composition and rate of growth of *Patella coerulea*, *Monodonta turbinata* and *M. articulata* shells from the western coast of sicily. Palaeogeogr. Palaeoclimatol. Palaeoecol. 42, 305–311. https://doi.org/10.1016/0031-0182(83)90028-7.

Schöne, B., 2008. The curse of physiology—challenges and opportunities in the interpretation of geochemical data from mollusk shells. Geo-Mar. Lett. 28, 269–285. https://doi.org/10.1007/s00367-008-0114-6.

Schöne, B.R., 2003. A "clam-ring" master-chronology constructed from a short-lived bivalve mollusc from the northern Gulf of California, USA. The Holocene 13 (1), 39–49. https://doi.org/10.1191/0959683603hl593rp.

Schöne, B.R., 2013. Arctica islandica (Bivalvia): a unique paleoenvironmental archive of the northern North Atlantic Ocean. Glob. Planet. Chang. 111, 199–225. https://doi.org/10.1016/j.gloplacha.2013.09.013.

Schöne, B.R., Dunca, E., Fiebig, J., Pfeiffer, M., 2005. Mutvei's solution: an ideal agent for resolving microgrowth structures of biogenic carbonates. Palaeogeogr. Palaeoclimatol. Palaeoecol. 228, 149–166. https://doi.org/10.1016/j.palaeo.2005.03.054.

Shackleton, N.J., 1973. Oxygen isotope analysis as a means of determining season of occupation of prehistoric midden sites. Archaeometry 15 (1), 133–141. https://doi.org/10.1111/j.1475-4754.1973.tb00082.x.

Wanamaker Jr., A.D., Kreutz, K.J., Borns Jr., H.W., Introne, D.S., Feindel, S., Barber, B.J., 2006. An aquaculture-based method for calibrated bivalve isotope paleothermometry. Geochem. Geophys. Geosyst. 7, Q09011. https://doi.org/10.1029/2005GC001189.

Wang, T., Surge, D., Walker, K.J., 2013. Seasonal climate change across the Roman warm period/Vandal Minimum transition using isotope sclerochronology in archaeological shells and otoliths, Southwest Florida, USA. Quat. Int. 308-309, 230–241. https://doi.org/10.1016/j.quaint.2012.11.013.

Zilhão, J., Angelucci, D.E., Badal-García, E., d'Errico, F., Daniel, F., Dayet, L., Douka, K., Higham, T.F.G., Martínez-Sánchez, M.J., Montes-Bernárdez, R., Murcia-Mascarós, S., Pérez-Sirvent, C., Roldán-García, C., Vanhaeren, M., Villaverde, V., Wood, R., Zapata, J., 2010. Symbolic use of marine shells and mineral pigments by Iberian Neandertals. Proc. Natl. Acad. Sci. 107, 1023–1028. https://doi.org/10.1073/pnas.0914088107.